

INVESTIGATIONS OF THE $\text{TlInP}_2\text{Se}_6\text{--In}_4(\text{P}_2\text{Se}_6)_3$ SYSTEM AND ITS OPTICAL PROPERTIES

VALERIA TOVT,¹ IGOR BARCHIY,^{1*} MICHAL PIASECKI,² IWAN KITYK,³ AND ANATOLII FEDORCHUK⁴

¹ Department of Chemistry, Uzhgorod National University, Pidgirna St. 46, 88000 Uzhgorod, UKRAINE

² Institute of Physics, Jan Dlugosz University, Armii Krajowej 13/15, 42-200 Częstochowa, POLAND

³ Faculty of Electrical Engineering, Częstochowa University of Technology, Dabrowskiego 69, 42201 Częstochowa, POLAND

⁴ Department of Inorganic and Organic Chemistry, Lviv National University of Veterinary Medicine and Biotechnologies, Pekarska St. 50, 79010 Lviv, UKRAINE

The equilibrium phases were investigated and the corresponding phase diagram constructed for the $\text{TlInP}_2\text{Se}_6\text{--In}_4(\text{P}_2\text{Se}_6)_3$ system from physical and chemical analyses, namely differential thermal analysis (DTA), X-ray diffraction (XRD), and microstructural analysis (MSA). It was established that this system belongs to the eutectic type and is characterized by the formation of boundary solid phases containing complex compounds. Single crystals of the compounds $\text{TlInP}_2\text{Se}_6$ and $\text{In}_4(\text{P}_2\text{Se}_6)_3$ were grown using the Bridgman method. Both crystals were found to exhibit diffuse reflection spectra and photoinduced dependence of birefringence at various IR wavelengths generated by CO_2 laser irradiation. Birefringence properties were investigated using the Senarmont method.

Keywords: phase diagram, solid solution, crystal structure, optical properties, direct-gap semiconductor, indirect-gap semiconductor, photoinduced birefringence

1. Introduction

Compounds with the formula $\text{M}_2\text{P}_2\text{Se}_6$ possess promising magneto-electric, piezoelectric, electro-optical, and thermoelectric properties that indicate their suitability as functional materials in optoelectronics [1-2]. Due to their crystal structure, they exhibit anisotropy in terms of their physical properties. In a multilevel structure of $\text{M}_2\text{P}_2\text{Se}_6$ compounds, metal cations and pairs of phosphorous atoms occupy the octahedral positions between planes of selenium atoms. This structure is characterized by its layered arrangement of atoms, which contributes to the formation of a dipole moment between the layers of cationic and anionic groups. The replacement of the metal cation M^{2+} by other metal cations (M^+ , M^{3+} or M^{4+}) leads to the deformation of the structure [3-4], changes the magnitude of the dipole moment and, consequently, its physical properties.

The $\text{Tl}_2\text{Se--In}_2\text{Se}_3\text{--P}_2\text{Se}_4$ ternary system is composed of binary $\text{Tl}_2\text{Se--In}_2\text{Se}_3$, $\text{Tl}_2\text{Se--P}_2\text{Se}_4$ and $\text{In}_2\text{Se}_3\text{--P}_2\text{Se}_4$ systems. The $\text{Tl}_2\text{Se--In}_2\text{Se}_3$ system is characterized by the formation of two intermediate ternary compounds: TlInSe_2 melts congruently at 1023 K and TlIn_5Se_8 is formed according to the peritectic reaction $\text{L} + \text{In}_2\text{Se}_3 \leftrightarrow \text{TlIn}_5\text{Se}_8$ at 1029 K [5-6]. In the sys-

tem $\text{Tl}_2\text{Se--P}_2\text{Se}_4$ with a ratio of 2 to 1, interoperable components form the compound $\text{Tl}_4\text{P}_2\text{Se}_6$ which possesses a congruent nature of melting at 758 K [7]. The $\text{In}_2\text{Se}_3\text{--P}_2\text{Se}_4$ system is characterized by the formation of the compound $\text{In}_4(\text{P}_2\text{Se}_6)_3$ in a syntectic reaction of $\text{L1} + \text{L2} \leftrightarrow \text{In}_4(\text{P}_2\text{Se}_6)_3$ at 880 K [8]. In the $\text{Tl}_2\text{Se--In}_2\text{Se}_3\text{--P}_2\text{Se}_4$ system at the intersection of incisions, the phases $\text{Tl}_4\text{P}_2\text{Se}_6\text{--In}_4(\text{P}_2\text{Se}_6)_3$ and $\text{TlInSe}_2\text{--P}_2\text{Se}_4$ form the complex compound $\text{TlInP}_2\text{Se}_6$ [9].

2. Experimental

Ternary $\text{Tl}_4\text{P}_2\text{Se}_6$ and $\text{In}_4(\text{P}_2\text{Se}_6)_3$ compounds were prepared by melting stoichiometric quantities of binary Tl_2Se with elementary indium, phosphorous and selenium under a vacuum of 0.13 Pa in quartz ampoules using a single temperature method. In all syntheses, components were used that possess a purity greater than 99.999%. The maximum temperatures of synthesis were 993 and 893 K for $\text{In}_4(\text{P}_2\text{Se}_6)_3$ and $\text{TlInP}_2\text{Se}_6$, respectively. The rate of heating up to the maximum temperature was 50 K h^{-1} . The melts were maintained at the maximum temperature for 72 hours. Cooling was performed at a rate of 50 K h^{-1} down to an annealing temperature of 573 K. The linearity of the heating and cooling processes was achieved by a RIF-101 temperature controller. The homogenization process occurred over 120 hours. Identification of the complex compounds and alloys was conducted by differential thermal analy-

*Correspondence: i_barchiy@ukr.net

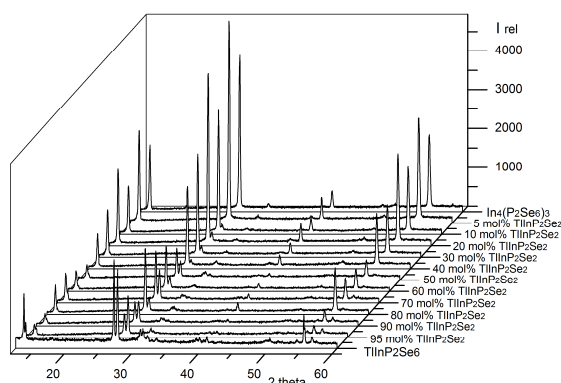


Figure 1. Results of the XRD analysis of the $\text{TlInP}_2\text{Se}_6\text{-In}_4(\text{P}_2\text{Se}_6)_3$ system. (I rel – Intensity, 2 theta – Angle of reflection)

sis (DTA) (PRA-01, chrome-alumina thermocouple ± 5 K), X-ray diffraction (XRD) (DRON-3 diffractometer, $\text{CuK}\alpha$ radiation, Ni filter) and microstructural analysis (MSA) (metallurgical microscope Lomo Metam R-1). Crystal structural calculations were conducted using the software package WinCSD [10]. Optical properties were investigated using an SF-18 spectrophotometer within the wavelength range of 400 – 750 nm. A CO_2 laser was used for photoinduced electrons in samples employing 200 ns pulses with a pulse repetition frequency of about 10 Hz, a fundamental frequency of 10.6 μm and a frequency doubling of 5.3 μm beams. The birefringence was measured using a Er:glass cw laser at 1540 nm by application of the Senarmont method.

3. Results and Analysis

3.1. Phase diagram of the $\text{TlInP}_2\text{Se}_6\text{-In}_4(\text{P}_2\text{Se}_6)_3$ system

The $\text{TlInP}_2\text{Se}_6\text{-In}_4(\text{P}_2\text{Se}_6)_3$ system is a quasi-binary section of the $\text{Tl}_2\text{Se-In}_2\text{Se}_3\text{-P}_2\text{Se}_4$ ternary system (Figs. 1 and 2). It belongs to the eutectic type (V-type diagram by Rozeboom). The complex compounds $\text{TlInP}_2\text{Se}_6$ and $\text{In}_4(\text{P}_2\text{Se}_6)_3$ melt congruently at 875 K and 963 K, respectively. $\text{TlInP}_2\text{Se}_6$ is characterized by two polymorphic transformations $lt\text{TlInP}_2\text{Se}_6 \leftrightarrow mt\text{TlInP}_2\text{Se}_6$ at 680 K and $mt\text{TlInP}_2\text{Se}_6 \leftrightarrow ht\text{TlInP}_2\text{Se}_6$ at 711 K. The prefixes *lt*-, *mt*- and *ht*- represent low-, medium-, and high-temperature modifications, respectively. $\text{In}_4(\text{P}_2\text{Se}_6)_3$ is also characterized by two polymorphic transformations $lt\text{In}_4(\text{P}_2\text{Se}_6)_3 \leftrightarrow mt\text{In}_4(\text{P}_2\text{Se}_6)_3$ at 665 K and $mt\text{In}_4(\text{P}_2\text{Se}_6)_3 \leftrightarrow ht\text{In}_4(\text{P}_2\text{Se}_6)_3$ at 903 K. When the temperature rises above 791 K, an invariant eutectic process is observed $\text{L} \leftrightarrow ht\text{TlInP}_2\text{Se}_6 + mt\text{In}_4(\text{P}_2\text{Se}_6)_3$ (in

Table 1. Crystal data of $\text{TlInP}_2\text{Se}_6$ and $\text{In}_4(\text{P}_2\text{Se}_6)_3$ compounds.

Compound	Crystal system	Space group	Lattice constant
$\text{In}_4(\text{P}_2\text{Se}_6)_3$ [8]	trigonal	$R\bar{3}h$ (146)	$a = 6.362(3)$, $c = 19.929(6)$ Å
$\text{In}_4(\text{P}_2\text{Se}_6)_3$	trigonal	$R\bar{3}h$ (146)	$a = 6.3808(8)$, $c = 20.014(4)$ Å
$\text{TlInP}_2\text{Se}_6$ [2]	triclinic	$P\bar{1}$ (2)	$a = 6.4310$, $b = 7.5002$, $c = 12.124$ Å,
$\text{TlInP}_2\text{Se}_6$	triclinic	$P\bar{1}$ (2)	$\alpha = 100.553$, $\beta = 93.735$, $\gamma = 113.451$

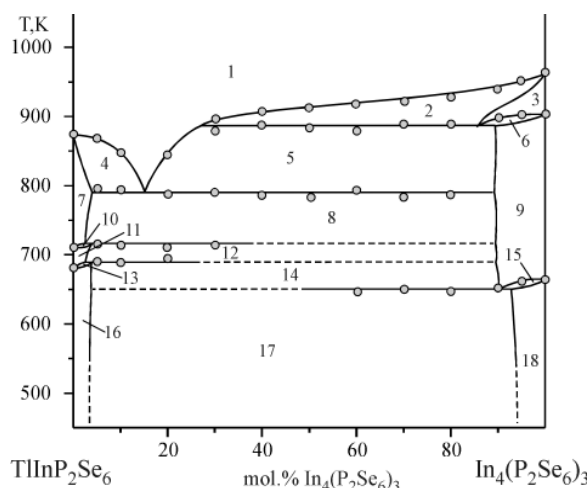


Figure 2. Phase diagram of the $\text{TlInP}_2\text{Se}_6\text{-In}_4(\text{P}_2\text{Se}_6)_3$ system. (1–L, 2–L+*ht* $\text{In}_4(\text{P}_2\text{Se}_6)_3$, 3–*ht* $\text{In}_4(\text{P}_2\text{Se}_6)_3$, 4–*ht* $\text{TlInP}_2\text{Se}_6$, 5–L+*mt* $\text{In}_4(\text{P}_2\text{Se}_6)_3$, 6–*ht* $\text{In}_4(\text{P}_2\text{Se}_6)_3$ +*mt* $\text{In}_4(\text{P}_2\text{Se}_6)_3$, 7–*ht* $\text{TlInP}_2\text{Se}_6$, 8–*ht* $\text{TlInP}_2\text{Se}_6$ +*mt* $\text{In}_4(\text{P}_2\text{Se}_6)_3$, 9–*mt* $\text{In}_4(\text{P}_2\text{Se}_6)_3$, 10–*ht* $\text{TlInP}_2\text{Se}_6$ +*mt* $\text{TlInP}_2\text{Se}_6$, 11–*mt* $\text{TlInP}_2\text{Se}_6$, 12–*mt* $\text{TlInP}_2\text{Se}_6$ +*mt* $\text{In}_4(\text{P}_2\text{Se}_6)_3$, 13–*mt* $\text{TlInP}_2\text{Se}_6$ +*lt* $\text{TlInP}_2\text{Se}_6$, 14–*lt* $\text{TlInP}_2\text{Se}_6$ +*mt* $\text{In}_4(\text{P}_2\text{Se}_6)_3$, 15–*mt* $\text{In}_4(\text{P}_2\text{Se}_6)_3$ +*lt* $\text{In}_4(\text{P}_2\text{Se}_6)_3$, 16–*lt* $\text{TlInP}_2\text{Se}_6$, 17–*lt* $\text{TlInP}_2\text{Se}_6$ +*lt* $\text{In}_4(\text{P}_2\text{Se}_6)_3$, 18–*lt* $\text{In}_4(\text{P}_2\text{Se}_6)_3$).

the presence of 15 mol% $\text{In}_4(\text{P}_2\text{Se}_6)_3$).

The system is described by the sequence of the efficient peritectic processes $ht\text{TlInP}_2\text{Se}_6 + mt\text{In}_4(\text{P}_2\text{Se}_6)_3 \leftrightarrow mt\text{TlInP}_2\text{Se}_6$ (714 K) and $mt\text{TlInP}_2\text{Se}_6 + mt\text{In}_4(\text{P}_2\text{Se}_6)_3 \leftrightarrow lt\text{TlInP}_2\text{Se}_6$ (689 K) based on the polymorphic transformation of $\text{TlInP}_2\text{Se}_6$. The polymorphism of $\text{In}_4(\text{P}_2\text{Se}_6)_3$ produces metatectic $ht\text{In}_4(\text{P}_2\text{Se}_6)_3 \leftrightarrow \text{L} + mt\text{In}_4(\text{P}_2\text{Se}_6)_3$ (884 K) and eutectic $mt\text{In}_4(\text{P}_2\text{Se}_6)_3 \leftrightarrow lt\text{TlInP}_2\text{Se}_6 + lt\text{In}_4(\text{P}_2\text{Se}_6)_3$ (652 K) processes. Regions of homogeneity in solid solutions, based on the batched complex selenides during annealing at a temperature of 573 K, do not exceed 10 mol%.

3.2. Crystal structure of the compounds $\text{In}_4(\text{P}_2\text{Se}_6)_3$ and $\text{TlInP}_2\text{Se}_6$

The crystal structures of the compounds $\text{TlInP}_2\text{Se}_6$ and $\text{In}_4(\text{P}_2\text{Se}_6)_3$ were solved using the Rietveld method. As an initial model for $\text{TlInP}_2\text{Se}_6$ [2], the parameters of $\text{In}_4(\text{P}_2\text{Se}_6)_3$ were used [8]. Analysis of the crystalline structures of the investigated compounds (Table 1) showed that it is possible to define the structural group of the anionic group $[\text{P}_2\text{Se}_6]^{4-}$, which is formed by two single tetrahedra (Fig. 3). Cationic atoms occupy positions between the anionic groups and none are located between the layers.

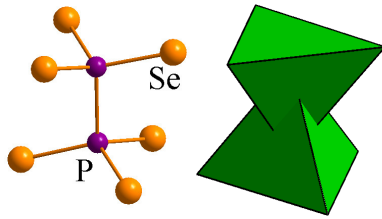


Figure 3. Structure of the anionic group $[\text{P}_2\text{Se}_6]^{4-}$.

The structure of $\text{In}_4(\text{P}_2\text{Se}_6)_3$ can be derived from the structure of $\text{Sn}_2\text{P}_2\text{Se}_6$ [11]. It is composed of multiple substitutions of the isovalent cations according to $2\text{M}^{2+} \leftrightarrow \text{M}^{4+}$. The crystal structure of the compound $\text{In}_4(\text{P}_2\text{Se}_6)_3$ can be presented based on the composition of the anionic group $[\text{P}_2\text{Se}_6]^{4-}$ (Fig. 4), in which the indium atoms occupy the space between the anionic groups.

The second coordination environment (SCE) [12] is of cuboctahedron form. Indium cations are surrounded by a triangular environment of anionic atoms of the group $[\text{P}_2\text{Se}_6]^{4-}$ and within the frames of its environment bonding exists with six atoms of selenium while the coordination form is octahedral (Fig. 5).

The structural and chemical properties of the $\text{Me}^{\text{I}}\text{Me}^{\text{II}}\text{P}_2\text{Se}_6$ compositions are related to the important role concerning the dimension of the cation on its location between the layers of the anionic $[\text{P}_2\text{Se}_6]^{4-}$ groups. Crystallographic analysis showed that smaller cations occupy a position in the plane perpendicular to the main axis. Atoms located in a second coordination environment of anionic groups in the structure of $\text{TlInP}_2\text{Se}_6$ compounds can be presented as a strongly distorted hexagonal-equivalent cuboctahedron (Fig. 6).

The atoms of metallic cations, located in the cavities between the atoms of the anionic groups, are within an asymmetric environment (Fig. 7). In^{3+} cations move toward tetrahedral cavities on the boundary between

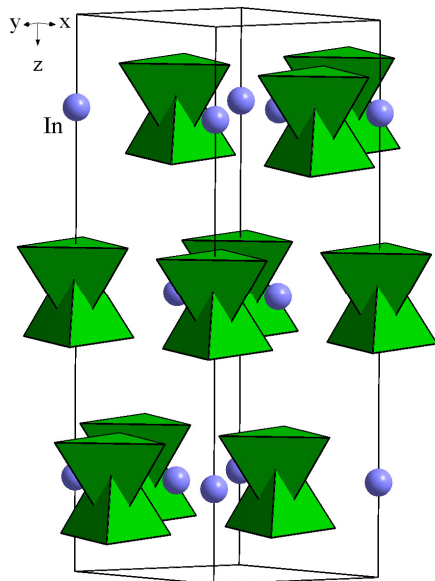


Figure 4. Arrangement of the polyhedra anionic group $[\text{P}_2\text{Se}_6]^{4-}$ in $\text{In}_4(\text{P}_2\text{Se}_6)_3$.

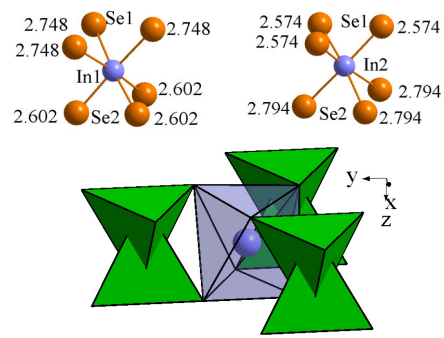


Figure 5. Coordination environment of the indium atoms in the structure of $\text{In}_4(\text{P}_2\text{Se}_6)_3$.

tetrahedral and octahedral cavities, and Tl^+ cations move in the direction of the octahedral cavities.

Moreover the In^{3+} cations are located in the same plane together with the centres of the anionic $[\text{P}_2\text{Se}_6]^{4-}$ groups (Fig. 8) and some Tl^+ cations are shifted relative to the plane. Therefore, this arrangement is a source of the interesting electro-physical and optical properties of materials based on compounds of this type.

3.3. Optical response of single crystals of $\text{TlInP}_2\text{Se}_6$ and $\text{In}_4(\text{P}_2\text{Se}_6)_3$

The most important parameter of the energy spectra of semiconductors is the width of the band gap, E_g , which is defined by the difference in energy between the bottom of the conduction band, E_C , and the top of the valence band, E_V . All semiconductors can be divided into two groups. In the first group, the minimum of the conduction band and the maximum of the valence band occupy the same point in the Brillouin zone, i.e. at an identical location in the space of quasi-moments. In this case, the optical transitions of electrons from the valence band to the conduction band (with the absorption of a quantum of light) and from the conduction band to the valence band (with the emission of a quantum of light) occur so that the electrons practically do not change their quasi-moments. Such transitions are characteristic of direct-gap semiconductors. For the second group, the absolute minimum of the conduction band and the absolute maximum of the valence band are at different points in the Brillouin zone, and optical inter-

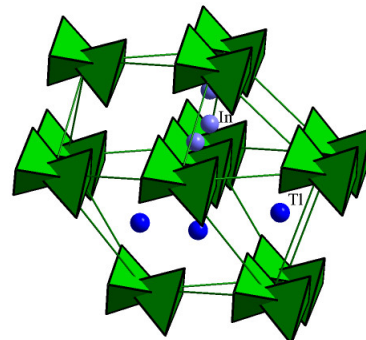


Figure 6. Second (SCE) and nearest (NCE) coordination environments of atoms in the $[\text{P}_2\text{Se}_6]^{4-}$ anionic groups in the structure of $\text{TlInP}_2\text{Se}_6$.

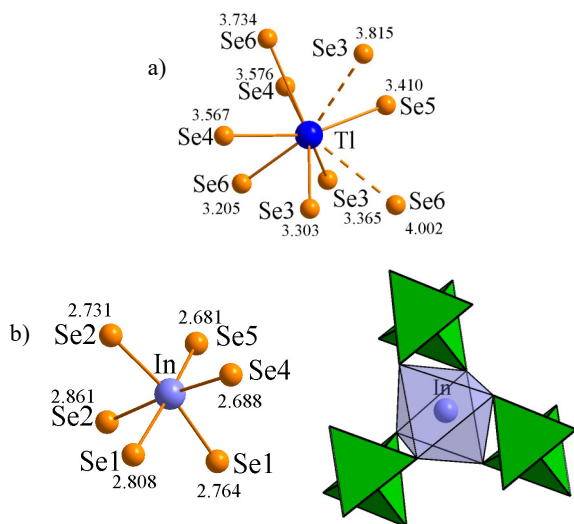


Figure 7. Coordination environments of the thallium (a) and indium (b) atoms in the structure of $\text{TlInP}_2\text{Se}_6$.

band transitions must be accompanied by a large change in the electron quasi-moment. These are characteristic of indirect-gap semiconductors. Since the photon moment is negligibly small compared with the electron quasi-moment, the latter case is possible only when the electron interacts with the phonon.

According to the phase diagram, the single crystals of $\text{TlInP}_2\text{Se}_6$ and $\text{In}_4(\text{P}_2\text{Se}_6)_3$ were grown using the Bridgman method in two vertical zone furnaces. Experimental studies of optical spectra in the absorption region yielded information on the energy spectrum of electrons near the edges of the conduction band and band gap. Studies concerning the dependence of diffuse reflection on wavelength ($R = f(\lambda)$) have shown that the compound $\text{TlInP}_2\text{Se}_6$ refers to indirect-gap semiconductors. On the graph there are two rectilinear sections, one of which (for small wavelengths, λ , and large values of E) characterizes the interband transitions of electrons with phonon emission, and the other (for large λ and small E) describes the processes of phonon absorption (Fig. 9).

The intersection of the first section with the wavelength axis, λ , yields the value of $E_g + E_{\text{phonon}}$ ($\lambda = 560$ nm, $E = 2.21$ eV), and the intersection of the second

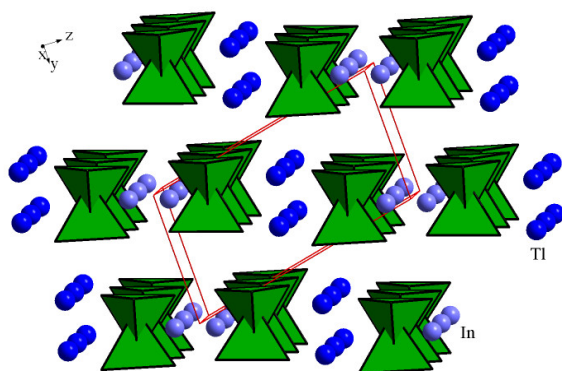


Figure 8. Arrangement of the polyhedra anionic group $[\text{P}_2\text{Se}_6]^{4-}$ in the structure of $\text{TlInP}_2\text{Se}_6$.

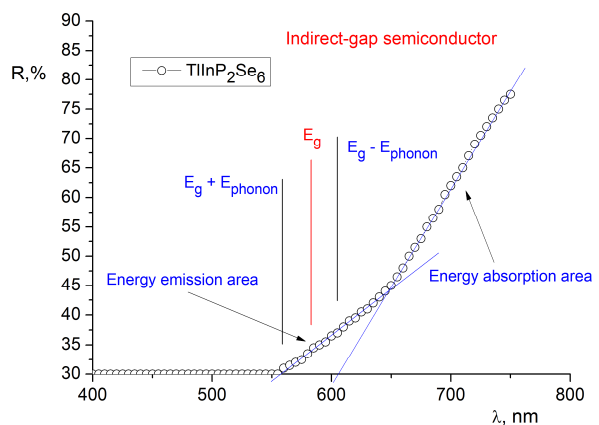


Figure 9. Dependence of the diffuse reflection R on the wavelength λ for the compound $\text{TlInP}_2\text{Se}_6$.

characterizes $E_g - E_{\text{phonon}}$ ($\lambda = 605$ nm and $E = 2.05$ eV). The length of the segment between the points of intersection of both straight lines with the wavelength axis, λ , is equal to the doubled energy of the phonons, $2E_{\text{phonon}}$ (0.16 eV), interacting with the electron. The middle of this segment corresponds to the photon energy equal to the width of the band gap of the indirect-gap semiconductor, E_g . Experimental calculations in terms of the compound $\text{TlInP}_2\text{Se}_6$ have shown that $E_g = 2.13$ eV and $E_{\text{phonon}} = 0.08$ eV.

The compound $\text{In}_4(\text{P}_2\text{Se}_6)_3$ refers to direct-gap semiconductors, which characterizes the interband transitions of electrons in terms of photon absorption (Fig. 10). The intersection of the line with the wavelength axis, λ ($\lambda = 651$ nm), yields the value of $E_g = 1.91$ eV.

The crystals of $\text{In}_4(\text{P}_2\text{Se}_6)_3$ and $\text{TlInP}_2\text{Se}_6$ were illuminated by 10.6 μm and (its second harmonic) frequency doubling of 5.3 μm beams. Each channel of the beam was split by 200-ns CO_2 laser pulses with a pulse repetition frequency of about 10 Hz. The angle between these two laser beams was changed from 18° to 22° . Figs. 11 and 12 present these dependences. Treatment with a 10.6 μm beam achieved a smaller maximum birefringence (about 1.55×10^{-2}) in comparison to the 5.2 μm beam. This indicates a different photoinduced anisotropy for the $\text{In}_4(\text{P}_2\text{Se}_6)_3$ and $\text{TlInP}_2\text{Se}_6$ crystals. Because

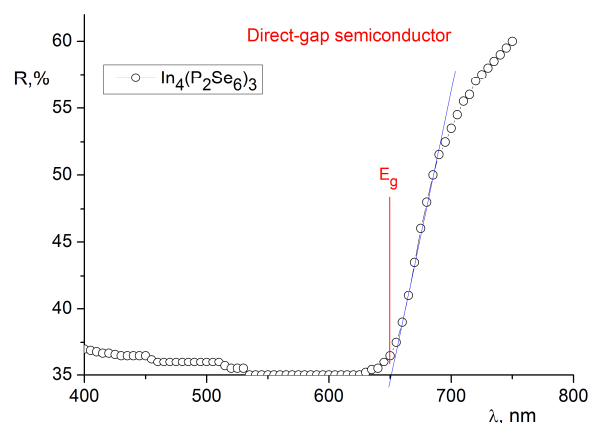


Figure 10. Dependence of the diffuse reflection R on the wavelength λ for the compound $\text{In}_4(\text{P}_2\text{Se}_6)_3$.

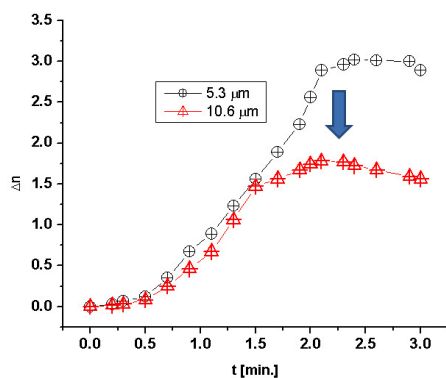


Figure 11. Photoinduced birefringence dependence at wavelengths of 5.3 μm and 10.6 μm - the two coherent beams were illuminated under different angles. During the two-beam coherent treatment at optimal power densities (about 400 MW/cm^2) and incident angles (18-22 degrees) for crystals of $\text{In}_4(\text{P}_2\text{Se}_6)_3$. The birefringence scale should be multiplied by 10^{-2} .

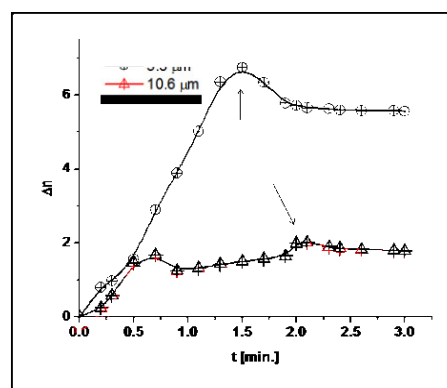


Figure 12. Photoinduced birefringence dependence at wavelengths of 5.3 μm and 10.6 μm - the two coherent beams were illuminated under different angles. During the two-beam coherent treatment at optimal power densities (about 400 MW/cm^2) and incident angles (18-22 degrees) for crystals of $\text{TlInP}_2\text{Se}_6$. The birefringence scale should be multiplied by 10^{-2} .

these crystals contain chalcogenide anions that contribute to the anharmonicity of the phonon, they play a crucial role in terms of the second harmonic generation [13-14]. The maximum changes in the birefringence achieved were less than 2×10^{-2} and 6.3×10^{-2} for CO_2 laser wavelengths of 10.6 μm and 5.3 μm , respectively.

4. Conclusion

Differential thermal analysis, X-ray diffraction and microstructural analysis were used to construct a phase diagram for the $\text{TlInP}_2\text{Se}_6\text{-In}_4(\text{P}_2\text{Se}_6)_3$ system, which can be characterized by a eutectic-type interaction. The invariant eutectic process $\text{L} \leftrightarrow \text{htTlInP}_2\text{Se}_6 + \text{mtIn}_4(\text{P}_2\text{Se}_6)_3$ (15 mol% $\text{In}_4(\text{P}_2\text{Se}_6)_3$) occurs at 791 K. Two polymorphic transformations were identified for $\text{TlInP}_2\text{Se}_6$ at 680 K and 711 K and for $\text{In}_4(\text{P}_2\text{Se}_6)_3$ at 665 K and 903 K. New compounds were not detected in the binary system. The regions of solid phases of the complex compounds $\text{TlInP}_2\text{Se}_6$ and $\text{In}_4(\text{P}_2\text{Se}_6)_3$ do not exceed 10 mol%. Single crystals of both test compounds were achieved by the Bridgman method. Investigations concerning the dependence of the diffuse reflection spectrum showed that the compound $\text{TlInP}_2\text{Se}_6$ is characteristic of indirect-gap semiconductors ($E_g = 2.13$ eV, $E_{\text{phonon}} = 0.08$ eV), while the compound $\text{In}_4(\text{P}_2\text{Se}_6)_3$ is characteristic of direct-gap semiconductors ($E_g = 1.91$ eV, $E_{\text{phonon}} = 0.08$ eV). The dependence of the birefringence was photoinduced by wavelengths of 5.3 μm and 10.6 μm , which is indicative of different photoinduced anisotropy.

Acknowledgement

We are grateful for the financial support of this work by the Ministry of Education and Science of Ukraine under the project DB874P_0117U000380.

SYMBOLS

<i>ht</i>	high-temperature modification
<i>mt</i>	middle-temperature modification
<i>lt</i>	low-temperature modification
<i>SCE</i>	second coordination environment
<i>NCE</i>	nearest coordination environment
E_g	band gap, eV
E_{phonon}	phonon energy, eV
<i>R</i>	diffuse reflection
λ	wavelength, nm

REFERENCES

- [1] Galdamez, A., Manriquez, V., Kasaneva, J., Avila, R.E.: Synthesis, characterization and electrical properties of quaternary selenodiphosphates: AMP_2Se_6 with A – Cu, Ag and M – Bi, Sb, *Mat. Res. Bull.*, 2003 **38**, 1063-1072 DOI: 10.1016/S0025-5408(03)00068-0
- [2] McGuire, M.A.; Reynolds, T.K.; Di Salvo, F.J.: Exploring thallium compounds as thermoelectric materials: seventeen new thallium chalcogenides, *Chem. Mater.*, 2005 **17**, 2875-2884 DOI: 10.1021/cm050412c
- [3] Gave, M.A.; Bilc, D.; Mahanti, S.D.; Breshears, J.D.; Kanatzidis, M.G.: On the lamellar compounds $\text{CuBiP}_2\text{Se}_6$, $\text{AgBiP}_2\text{Se}_6$ and AgBiP_2S_6 . antiferroelectric phase transitions due to cooperative Cu^+ and Bi^{3+} ion motion, *Inorg. Chem.*, 2005 **44**, 5293-5303 DOI: 10.1021/ic050357
- [4] Pfeiff, R.; Kniep, R.: Quaternary selenodiphosphates(IV): $\text{M(I)M(III)[P}_2\text{Se}_6]$, (M(I) = Cu, Ag; M(III) = Cr, Al, Ga, In), *J. Alloys Compd.*, 1992 **186**, 111-133 DOI: 10.1016/0925-8388(92)90626-K

- [5] Mucha, I.: Phase diagram for the quasi-binary thallium(I) selenide–indium(III) selenide system, *Thermochimica Acta*, 2012 **550**, 1–4 DOI: 10.1016/j.tca.2012.09.028
- [6] Guseinov, G.D.; Abdullaev, G.B.; Godzhaev, E.M.; Rzaeva, L.A.; Agaev, G.A.: Constitutional diagram and physical properties of thallium selenide–indium selenide pseudobinary system, *Mater. Res. Bull.*, 1972 **7(12)**, 1497–1503 DOI: 10.1016/0025-5408(72)90187-0
- [7] Brockner, W.; Ohse, L.; Pätzmann, U.; Eisenmann, B.; Schäfer, H.: Kristallstruktur und Schwingungsspektrum des Tetra-Thallium-Hexaselenidohypodiphosphates $Tl_4P_2Se_6$, *Z. Naturforsch. A*, 1985 **40**, 1248–1252
- [8] Voroshilov, Y.V.; Gebesh, V.Y.; Potorii, M.V.: Phase equilibria in the system In–P–Se and crystal structure of β - $In_4(P_2Se_6)_3$, *Inorg. Mater.*, 1991 **27**, 2141–2144
- [9] Tovt, V.A.; Barchiy, I.E.; Piasecki, M.; Kityk, I.V.; Fedorchuk, A.O.; Solomon, A.M.; Pogodin, A.I.: Triangulation of the Tl_2Se – In_2Se_3 –“ P_2Se_4 ” quasi-ternary system, *Nauch. Vestn. Uzhgorod. Univ. (Ser. Khim.)*, 2016 **35(2)**, 14–19 (in Russian)
- [10] Akselrud, L.; Grin, Y.: WinCSD: Software package for crystallographic calculations (Ver.4), *J. Appl. Crystallogr.*, 2014 **47**, 803–805 DOI: 10.1107/S1600576714001058
- [11] Israel, R.; De Gelder, R.; Smits, J.M.M.; Beurskens, P.T.; Eijt, S.W.H.; Rasing, T.H.; van Kempen, H.; Maior, M.M.; Motrya, S.F.: Crystal structures of di-tin-hexa(seleno)hypodiphosphate, $Sn_2P_2Se_6$, in the ferroelectric and paraelectric phase, *Z. Kristallogr.*, 1998 **213**, 34–41 DOI: 10.1524/zkri.1998.213.1.34
- [12] Fedorchuk, A.O.; Parasyuk, O.V.; Kityk, I.V.: Second anion coordination for wurtzite and sphalerite chalcogenide derivatives as a tool for the description of anion sub-lattice, *Mat. Chem. Phys.*, 2013 **139**, 92–99 DOI: 10.1016/j.matchemphys.2012.12.058
- [13] Kityk, I.V.: IR-stimulated second harmonic generation in Sb_2Te_2Se – BaF_2 – $PbCl_2$ glasses, *J. Modern Optics*, 2004 **51**, 1179–1189 DOI: 10.1080/09500340408230415
- [14] Kityk, I.V.: IR-induced second harmonic generation in Sb_2Te_3 – BaF_2 – $PbCl_2$ glasses, *J. Phys. Chem. B*, 2003 **107**, 10083–10087 DOI: 10.1021/jp030058a